Taylor & Francis
Taylor & Francis Group

Drying Technology
An International Journal

ISSN: 0737-3937 (Print) 1532-2300 (Online) Journal homepage: http://www.tandfonline.com/loi/ldrt20

Optimization of freezing parameters for freeze-drying mango (Mangifera indica L.) slices

Natalia A. Salazar, Catalina Alvarez & Carlos E. Orrego

DRYING TECHNOLOGY
https://doi.org/10.1080/07373937.2017.1315431

Taylor & Francis
Taylor & Francis Group

Check for updates

Optimization of freezing parameters for freeze-drying mango (*Mangifera indica* L.) slices

Natalia A. Salazar[a], Catalina Alvarez[a], and Carlos E. Orrego[b]

[a]Departamento de Ingeniería Química, Instituto de Biotecnología y Agroindustria, Universidad Nacional de Colombia Sede Manizales, Manizales, Colombia; [b]Departamento de Física y Química, Instituto de Biotecnología y Agroindustria, Universidad Nacional de Colombia Sede Manizales, Manizales, Colombia

ABSTRACT

Today, there is an increasing trend toward consuming healthful food products, and dried fruits are one option for obtaining desirable nutrition in dehydrated products. Proper drying method selection is important for minimizing quality losses. Lyophilization (freeze-drying), a technique that removes water by sublimation at low temperature, can produce excellent dried products. Fast vacuum induction during freezing has been proposed as a way to control ice nucleation and to obtain enhanced lyophilized pharmaceutical products. However, this technique has not yet been applied to food freeze-drying. The aim of this work was to evaluate the effects of the freezing rate (0.4, 0.25, and 0.1°C/min), the minimum chamber pressure during vacuum-induced surface freezing (900, 700, and 500 mTorr) and the sample temperature at which the induced vacuum was applied (0, −2, and −4°C) on the total process time, final moisture content, rehydration capacity, total color difference, and total polyphenol content during the lyophilization of mango (*Mangifera indica* L.) slices. A Box–Behnken design with three factors at three levels was used to design the experiments, to generate the polynomial equations relating the dependent and independent variables, and to determine the optimal operational conditions. The results highlight the reduction of total process time (30%) at high freezing rates and the influence of the tested operating conditions on freeze-drying optimization. It was found that the optimal conditions that satisfy commercial quality goals were pressure between 500 and 650 mTorr, temperature between −2 and 0°C, and freezing rate values close to 0.4°C/min.

ARTICLE HISTORY
Received 19 September 2016
Revised 22 March 2017
Accepted 27 March 2017

KEYWORDS
Freeze-drying; freezing rate; mango; quality parameters; vacuum-induced surface freezing

Introduction

Tropical fruits are tasty, aromatic, energy-dense, and rich in water, fiber, vitamins, and minerals.[1] One of the main issues with tropical fruit production is high loss during postharvest handling, storage, and distribution.[2,3]

The mango is a tropical fruit with economic importance in many countries. In Colombia, the fruit is mainly grown in the central region of the country, with 20% of the cultivated area represented by the Tommy Atkins mango variety.[4,5]

Drying is used in the food industry to ensure microbiological stability, reduce product deterioration due to chemical reactions, facilitate storage, and lower transportation costs. Because fruits and vegetables are sensitive to heat, the selection of a suitable drying technology is a challenging task.[6] In the case of mango, many efforts have been undertaken to study the effect of different techniques of drying to obtain better quality dried products.[7,8]

Lyophilization, also called freeze-drying, is a dehydration process for the long-term preservation of heat-sensitive foodstuffs and other biological materials. It is based on the phenomenon of sublimation, which minimizes structural changes and preserves the bioactive compounds and flavors of the dried product.[9] Lyophilization includes three main steps: product freezing, primary drying (removing the ice by direct sublimation under reduced pressure), and secondary drying (release of unfrozen water by desorption and diffusion).[10]

Freezing is the first operation of lyophilization, during which the ice is formed. The freezing process may be divided into three stages: (1) nucleation or initial crystal seed formation; (2) propagation or growth of ice crystals; and (3) recrystallization or maturation.[11] The freezing rate (*F*) is a determinant of the final properties of the dried product, as it influences the pore size after ice crystal sublimation.[12] Despite the

CONTACT Carlos E. Orrego ceorregoa@unal.edu.co Departamento de Física y Química, Instituto de Biotecnología y Agroindustria, Universidad Nacional de Colombia Sede Manizales, Km 7 Vía al aeropuerto, Campus La Nubia, Manizales, Caldas, Colombia.
Color versions of one or more of the figures in the article can be found online at www.tandfonline.com/ldrt.

importance of freezing step, it typically is not properly controlled in industrial food lyophilization research or practice, and there have been few studies regarding the effects of freezing variables on the freeze-drying process and on the final quality of the food product.[13]

In contrast, there are several studies in the pharmaceutical field concerning the manipulation of freezing variables. Some authors have shown that control of nucleation can effectively provide process benefits. A study by Kramer et al.[14] demonstrated that the sudden reduction and release of the absolute chamber pressure during freezing stage reduce the primary dying time of solutions of mannitol, sucrose, and glycerin. Oddone et al.[15] explained that with this technique, the surface freezing triggered by the vacuum allows the control of nucleation temperature without requiring the installation of additional devices in the freeze dryer and improves the freeze-dried product homogeneity.[16] Liu et al.[17] combined this method with annealing during freezing to obtain significant effects on the primary step rate and the lyophilized product quality.

The aim of this work is to evaluate the effects of freezing rate (F), vacuum-induced surface freezing (VISF) pressure (P), and temperature at which the vacuum-induced pressure is applied (T) on the total process time (TPT), the final moisture content (MC), product rehydration capacity (RC), total color difference (ΔE_{ab}), and total polyphenol content (TPC) of lyophilized mango (*Mangifera indica* L.) slices.

Materials and methods

Sample preparation

Fresh mango (Tommy Atkins variety) was purchased from a local market in Manizales, Colombia. Fruit selection was performed manually according to size, and the chosen fruits displayed lengths between 0.1 and 0.15 m, widths between 0.08 and 0.1 m, and an average weight of 550 g. The fruit texture was evaluated by pressing the fruit with the fingertips to produce concave deformations, and mangoes with quick recovery of their original shapes were selected.[18] Cleaning and sanitization were performed before peeling. Each mango was then cut lengthwise into several slices; the flesh was cut down to the seed, but the seed itself was not cut. The pulp color and maturity state were tested using the color scale chart shown in Fig. 1, and mangoes with pulp colors between 3 and 4 were selected. Each slice was then cut into cylindrical pieces of 6.5 g that were 0.006 m in height and 0.040 m in diameter.

Experimental design and statistical optimization

Response surface modeling (RSM) is a group of empirical techniques that are useful for establishing and optimizing functional relationships between response variables and a set of independent input variables. A Box–Behnken design (BBD) with three independent variables, namely, F, P, and T was studied. The design matrix for the BBD also included five replications on the central point, resulting in a total of 17 experiments. The response variables were TPT, MC, RC, (ΔE_{ab}), and TPC of the lyophilized mango slices. The ranges and levels of the three independent variables were selected based on the results obtained in the previous experiments[19] and are presented in Table 1.

Design-Expert version 9.0 (Stat-Ease Inc., Minneapolis, MN, USA) was used to generate the run order and to study how the independent variables affected the responses. Polynomial models were fitted to the data to establish correlations between the variables and each response. Multiple linear regression analysis of the experimental data was used to evaluate the statistical significance of the developed models. Analysis of variance (ANOVA) was also used to test the significance of the terms of each model, where an F-value (Fisher's variance value) higher than unity suggests that the factors adequately explain the variation in the data about its mean and that the effects of estimated factors are true. Input variables were evaluated under the model shown in Eq. (1)

$$Y = \beta_0 + \sum_{i=1}^{k} \beta_i x_i + \sum_{i=1}^{k} \beta_{ii} x^2 + \sum \sum_{i<1} \beta_{ij} x_i x_j + \varepsilon \quad (1)$$

where the response function (Y) was partitioned into linear (β_i), quadratic (β_{ii}), and interactive components (β_{ij}); x_i and x_j are the levels of response variables, k is

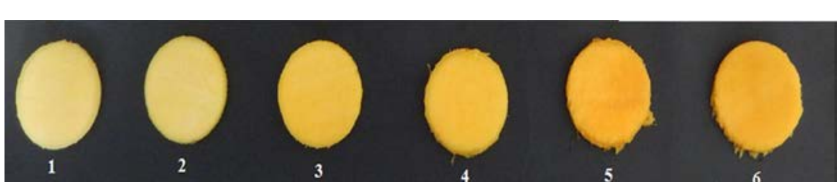

Figure 1. Color scale chart used to select mangoes.

Table 1. Levels of independent variables chosen for the experimental design during freezing.

Variable	Unit	Symbol	Levels −1	0	1
Freezing rate	°C/min	*F*	0.1	0.25	0.4
Pressure	mTorr	*P*	500	700	900
Temperature	°C	*T*	−4	−2	0

P, vacuum-induced surface freezing pressure. *T*, temperature at which the induced surface freezing pressure was applied.

the number of input variables (3), and ε is the standard random error.

The coefficients of determination (R^2 and adjusted R^2) and the absolute average deviation (AAD) were analyzed as criteria to evaluate the quality of the model. The AAD was calculated using the following equation (2):

$$\mathrm{AAD} = 100\left[\sum_{i=1}^{p}\frac{\left|Y_{i,\mathrm{exp}} - Y_{i,\mathrm{calc}}\right|/Y_{i,\mathrm{exp}}}{p}\right] \tag{2}$$

where $Y_{i,\mathrm{exp}}$ and $Y_{i,\mathrm{calc}}$ are the experimental and calculated responses, respectively, and p is the number of experimental runs.

The models were refined after nonsignificant coefficients were examined and manually eliminated. Most of the polynomial coefficients, with exception of the terms required to retain the hierarchy of the models, had p-values below 0.05.

All of the analyses of the dried mango slices (DMS) were performed in triplicate, and the results are expressed as the mean values ± standard deviation.

Vacuum-induced surface freezing

Vacuum-induced surface freezing was performed as previously described[14] with modifications. The freezing and lyophilization of mango slices (MS) were conducted in a Virtis Genesis SQ XL-70 lyophilizer (Virtis, Gardiner, NY, USA). The MS were placed on the shelves of the chamber at 20°C and frozen to *T* before being subjected to the established experimental design with respect to *F*, *P* and the moment of vacuum release during the VISF treatment. Then, freezing continues until −40°C. Independent variables were set according to the conditions listed in Table 1 using the freeze dryer controller system. Control tests were run for each freezing rate.

Freeze-drying procedure

After the freezing step, primary and secondary drying, all the runs were performed using the same temperature and vacuum profiles in the chamber. To control and monitor product temperature during drying, a thermocouple was placed in the samples on the tray. A constant difference between the capacitance and Pirani gauges was used to determine the freeze-drying end point.

After lyophilization, all of the dried samples were vacuum-packed in individual high-barrier plastic bags and stored in the dark at 4°C until analysis.

Moisture content

The moisture content of DMS was determined using the oven drying method described in AOAC (2000), Method 934.06.

Rehydration capacity

Rehydration experiments were performed according to a modified version of the methodology proposed by Mothibe et al.[20] DMS of 1 g was immersed in 100 mL of distilled water at 25°C. The sample was removed after 15 min and drained over a mesh for 2 min to eliminate superficial water. Subsequently, its weight was recorded. Rehydration capacity (RC), defined as the ratio of rehydrated sample weight to that of the dry sample, was calculated according to the following equation (3):

$$\mathrm{RC} = \frac{m_\mathrm{f}}{m_0}(3) \tag{3}$$

where m_f and m_0 are the final (after 15 min of soaking) and initial weights of the DMS, respectively.

Color

Mango slices and DMS colors were measured with a portable Konica Minolta spectrophotometric colorimeter (CR-700, Konika Minolta, Tokyo, Japan) in the CIELab color space. The parameters *a** (red-green dimension), *b** (yellow-blue dimension), and *L** (luminosity) were determined. The total color difference (ΔE_{ab}) was calculated as shown in Eq. (4). Measurements were taken on two equatorial sides of each sample, taking the average of the results as the reported value.

$$\Delta E_{\mathrm{ab}} = \sqrt{\left(L_\mathrm{f}^* - L_0^*\right)^2 + \left(a_\mathrm{f}^* - a_0^*\right)^2 + \left(b_\mathrm{f}^* - b_0^*\right)^2} \tag{4}$$

where the o and f subindices indicate the initial (fresh fruit) and final (DMS) values of the *a** and *b** parameters.

Total polyphenol content

Ultrasonic extraction

Each sample of DMS (0.150 ± 0.001 g) was mixed with 1 mL of a solution of etanol:hydrochloric acid:water

(93:1:6 v/v) in a Eppendorf tube.[21] The tube was submerged during 2 h in an ultrasonic bath (Elma E30H, Singen, Alemania) with 37 kHz and 240 W of power level.[22,23] The temperature of the ultrasonic bath was controlled in normal conditions (23–25°C). Then, the extract was centrifuged at 13500 rpm, during 20 min, the supernatant was collected and stored in an amber glass vial at 4°C, under dark conditions until analysis. The concentration of total phenolic compounds was expressed in milligram gallic acid equivalents (GAE) per gram of dried fruit.

Measurement of total polyphenol content

The TPC of the extract was measured by the colorimetric method of Folin–Ciocalteu with modifications.[24] Extract of 150 µL was mixed with 2.4 mL of distilled water, 150 µL of Folin–Ciocalteu solution (1N), and 300 µL of sodium carbonate (20% w/v). After 2 h of reaction under dark conditions, absorbance was measured at a wavelength of 765 nm in a spectrophotometer (UV/Visible-Model 6405, Jenway, Felsted, UK).

Electricity cost estimation

The electrical power consumption of the freeze dryer for each test was measured with an electrical clamp meter (model TMRS; Fluke Corporation, Everett, USA) for the TPT. It was calculated using Eq. (5):

$$\mathrm{EP} = \sum_{1}^{n} W_i \Delta t_i \tag{5}$$

where EP is the power (kWh), n is TPT/Δt_i, W_i is electrical power consumption (kW) in stage i, and Δt_i is (1/12) h.

Based on these data, the energy costs per run were calculated according to the local energy cost of US $0.12/kWh.

Results and discussion

Figure 2 depicts typical temperature and pressure profiles for the freezing and lyophilization steps of MS. For the lyophilization stage, the top lines indicate temperature (shelf and product), while the bottom lines indicate chamber pressure (Pirani and capacitance gauges). The F, namely, the slope of linear zone between initial freezing point and lowest temperature reached by the samples during freezing, was set at three different levels (0.10, 0.25, and 0.40°C/min). During the freezing period and for each F tested, VISF was used; in this process, vacuum was suddenly applied until the chamber reaches a certain absolute pressure (500 mTorr in Fig. 2; hereafter termed P), at which time the vacuum was released and freezing proceeded at atmospheric pressure. The TPT for each test was the sum of lyophilization time and freezing time.

A sharp reduction, in the sample temperature when the VISF process was applied, was noted. In the freeze-drying of various pharmaceutical solutions, similar behavior was observed during freezing, which led to the formation of more-ordered dendritic ice crystals owing to the evaporative water losses caused by such treatment.[15] Oddone et al.[25] analyzed the temperature drop during VISF and compare it with the process without application of controlled nucleation. The temperature differences were 10 and 5°C, without and with controlled nucleation, respectively. However, the effects of VISF on the lyophilization step of a structured solid food, such as, MS, were unknown. To study this problem, a three-factor, three-level Box–Behnken experimental design in combination with RSM was used.

A total of 17 experiments, including five replicates at the central point, was used to identify the significant correlations between three input variables and five response variables. The range of input variables for the lyophilization assays (which were based on the results of preliminary experiments) and the experimental data for the responses are presented in Table 2.

Table 3 shows the polynomial functions for each response. The R^2, adjusted R^2, and AAD values shown in Table 3 indicated that the model equations explained the real behavior of the systems and were suitable for interpolation in the experimental domain.

Total process time

In the quadratic polynomial model for TPT (Table 3), F and T had significant negative effects on TPT. Conversely, P was not found to be significant ($p > 0.05$).

Previous studies had reported the influence of F on the quality parameters of lyophilized fruit or fruit derivatives. An investigation into the influence of F and the ripeness state of fresh zucchini on the final appearance and texture concluded that F did not affect the final product quality but that fruit ripeness was relevant.[26] Ceballos et al.[9] studied the effects of different F values (0.5–3.1°C/min) on the quality parameters of freeze-dried soursop fruit pulp. However, to our knowledge, previous works have not examined the effects of different F values or VISF parameters on the TPT for solid fruits or foods.

F rise results in lower ice crystal size and long lasting sublimation process, because average pore size in freeze-dried product and ice crystal size in previous frozen

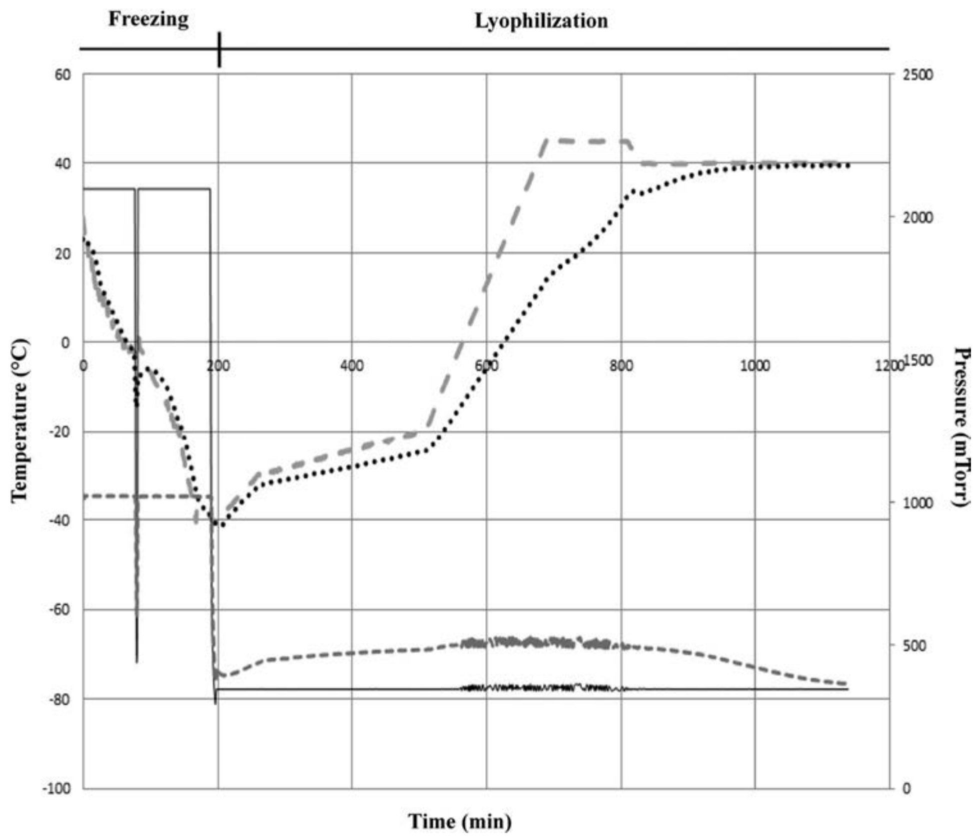

Figure 2. A typical freezing and lyophilization (primary and secondary drying) run with MS. – –, Shelf temperature; ····· mango temperature; —–, capacitance gauge; – – –, pirani gauge.

Table 2. Box–Behnken design factors and experimental data for MS freeze-drying.

	Input variables			Response variables			Color		
Exp	F^a (°C/min)	P^b (mTorr)	T^c (°C)	TPT (min)	Moisture (%)	Rehydration capacity	$(\Delta L^*)^d$	$(\Delta E_{ab})^e$	TPC (mg GAE/g dried fruit)
1	0.10	500	−2	1578	4.317 ± 0.146	3.486 ± 0.317	4.39 ± 0.80	5.44 ± 3.23	247.42 ± 88.96
2	0.25	700	−2	1195	3.706 ± 0.290	3.202 ± 0.335	−2.9 ± 0.03	4.39 ± 2.23	253.85 ± 49.28
3	0.40	700	0	1057	3.399 ± 0.139	3.543 ± 0.240	−6.05 ± 0.60	8.67 ± 2.91	243.38 ± 12.82
4	0.25	700	−2	1145	4.110 ± 0.129	3.465 ± 0.108	−1.7 ± 0.76	5.16 ± 3.19	285.83 ± 11.79
5	0.10	900	−2	1581	5.109 ± 0.573	2.468 ± 0.103	−5.82 ± 0.25	7.84 ± 4.79	183.73 ± 8.57
6	0.25	700	−2	1278	3.429 ± 0.296	3.566 ± 0.038	−2.85 ± 0.36	4.88 ± 1.86	281.26 ± 7.47
7	0.40	500	−2	1114	4.053 ± 0.399	3.583 ± 0.386	−0.85 ± 0.30	15.99 ± 2.75	334.43 ± 0.97
8	0.10	700	0	1500	5.235 ± 0.064	3.077 ± 0.059	−6.37 ± 0.35	7.33 ± 4.04	271.36 ± 9.40
9	0.10	700	−4	1513	4.365 ± 0.219	3.498 ± 0.145	−2.93 ± 0.17	9.27 ± 0.66	224.73 ± 20.03
10	0.40	900	−2	1142	4.644 ± 0.027	4.036 ± 0.152	−9.81 ± 0.91	22.59 ± 7.80	271.40 ± 20.39
11	0.25	500	−4	1209	2.965 ± 0.262	3.830 ± 0.063	−7.27 ± 0.08	8.46 ± 0.67	268.66 ± 25.69
12	0.40	700	−4	1065	3.220 ± 0.170	3.781 ± 0.204	0.92 ± 0.15	18.80 ± 6.13	256.35 ± 17.16
13	0.25	900	0	1206	3.450 ± 0.008	3.536 ± 0.232	−0.54 ± 0.21	11.84 ± 3.59	222.50 ± 16.83
14	0.25	700	−2	1264	4.088 ± 0.291	3.323 ± 0.077	−4.11 ± 0.59	4.68 ± 3.68	313.24 ± 56.89
15	0.25	700	−2	1317	4.082 ± 0.008	3.339 ± 0.048	−5.36 ± 0.84	8.47 ± 1.96	280.68 ± 30.71
16	0.25	500	0	1179	4.525 ± 0.290	3.311 ± 0.0092	0.33 ± 0.14	11.37 ± 4.40	415.38 ± 62.22
17	0.25	900	−4	1168	5.720 ± 0.382	3.801 ± 0.260	−12.48 ± 0.71	17.47 ± 2.20	304.16 ± 69.25

TPT, total process time; TPC, total polyphenol content; GAE, gallic acid equivalents; VISF, vacuum-induced surface freezing.
Except for the TPT, the response variable data represent the mean ± standard deviation of three measurements.
[a]The freezing rate is defined as the slope of the linear portion of the mango temperature profile, measured from the initial freezing to the lowest temperature reached during freezing.
[b]The minimum VISF reached during the freezing cycle.
[c]The temperature at which the induced vacuum is applied.
[d]Lightness difference ($L_f^* - L_0^*$) between fresh and DMS.
[e]Total color change.

Table 3. ANOVA results for response parameters.

Response	Final equation in terms of actual factors	Model	*p*-Value	LOF	R^2	Adj. R^2	AP	AAD
TPT[a]	$1846.47 - 59.92T - 3809.33F - 14.78T^2 + 4628.65F^2$	Quadratic	<0.0001	0.99	0.96	0.94	22.35	4.00
Moisture	$6.97 + 1.70T - 2.87 \times 10^{-3}P - 3.09F - 2.39 \times 10^{-3}TP$	Quadratic	0.0024	0.16	0.72	0.63	10.82	0.46
RC[b]	$5.08 - 0.09T - 3.29 \times 10^{-3}P - 6.56F + 0.01PF$	Quadratic	0.0006	0.22	0.78	0.71	12.95	0.35
ΔE_{ab}[c]	$54.80 - 0.15P - 41.35F + 1.12 \times 10^{-4}P^2 + 143.00F^2$	Quadratic	0.0031	0.05	0.71	0.61	8.57	1.71
PL[d]	$-7.04 - 23.93T + 0.10P - 252.90F + 0.03TP + 441.22F^2$	Quadratic	0.0003	0.25	0.85	0.78	14.34	0.71

ANOVA, analysis of variance; *p*-value, probability of error; LOF, lack of fit; Adj. R^2, adjusted R^2; AP, adequate precision; AAD, absolute average deviation.
[a]Total process time.
[b]Rehydration capacity.
[c]Total color change.
[d]Polyphenol losses.

product are about the same. This in turn reduces the water effective diffusivity, makes difficult, and slows the ice water sublimation. These principles are commonly accepted in food freeze-drying industry and the selection of a suitable *F* for the freeze-drying of a specific food has to consider, among other aspects, its effect on the sublimation rate, and the freezing and lyophilization times.

For the tests described in this paper, the lyophilization times (870–900 min) did not present significant differences, and TPT most clearly depended on the level of *F* in the freezing stage.

The RSM contour plots in Fig. 3 showed that when $F \leq 0.3$°C/min, there were local maximums of TPT at $T = -2$°C, and at $T = 0$°C or $T = -4$°C, the TPT response for identical *F* was nearly the same. At $F \geq 0.3$°C/min, the TPT reached its lower limit. Indeed, the model predicts the use of a high *F* (0.4°C/min) and a low *T* (−4°C) reduced TPT by as much as approximately 30% compared with the TPT at $F = 0.1$°C/min.

Moisture content

The moisture content of fresh mango slices showed little variability (83.75 ± 1.93% w.b.). The moisture content measurements for freeze-dried samples also displayed low to moderate variability, and their reproducibility was good, as evidenced by the close values for final

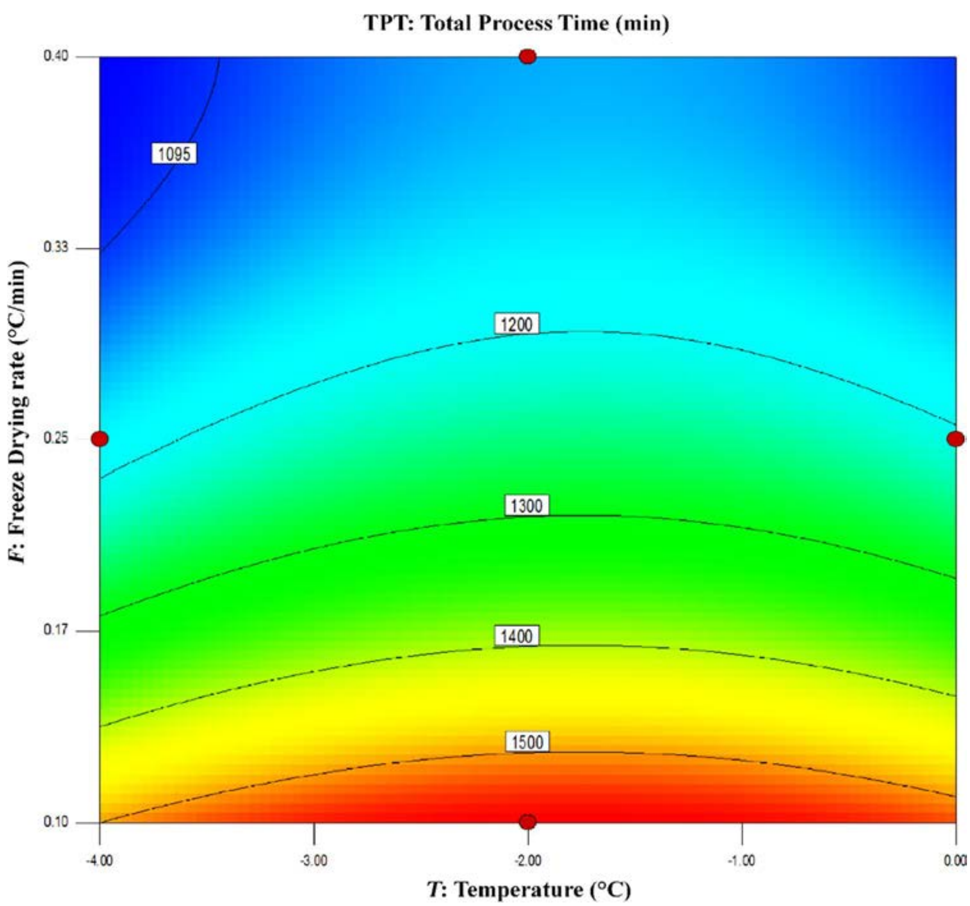

Figure 3. Response contour plot showing the effects of *F* and *T* on the TPT for $P = 900$ mTorr. *Note*: TPT, total process time.

moisture content in the dried samples from the central point of the experimental design (runs 2, 4, 6, 14, and 15 in Table 2). This is something remarkable, since the mango slices were not entirely homogeneous in terms of tissue structure or the fruit ripening stage. Furthermore, comparative pressure measurement used to state the end point of freeze-drying did not fully assured to meet such closer moisture uniformity. Apparently, the use of VISF contributed to this end moisture consistency.

After drying, the initial water content was reduced up to 70–80%. A comparable decrease was reported for the lyophilization of macerated mango pulp (73.07%).[27]

This parameter could also be modeled with a quadratic polynomial (Table 3). The most significant terms ($p < 0.001$) were *P*, *F* and the interaction $T*P$. The moisture content of dried samples obtained with different freezing rates ranged from 4.3 to 5.2%, 2.9 to 5.7%, and 3.2 to 4.6% for 0.1, 0.25, and 0.4°C/min, respectively. Thus, little greater product moisture contents were found when *F* was 0.1°C/min and $P = 900$ mtorr (Table 2 and Fig. 4). In the first situation, this apparently paradoxical result may be explained by the fact that the lyophilization times (data not shown)

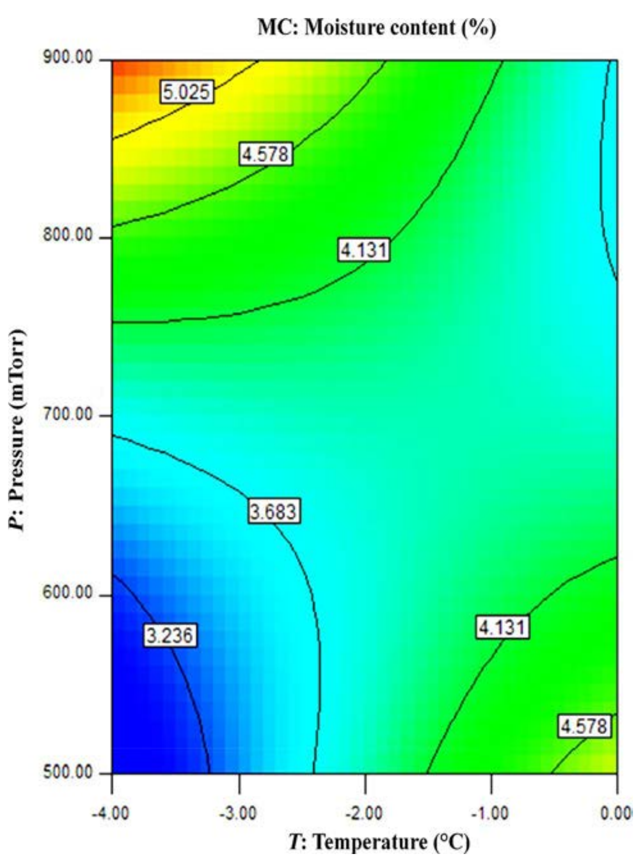

Figure 4. Contour plot showing the effects of *P* and *T* on the moisture content of DMS at a freezing rate of 0.25°C/min. *Note*: DMS, dried mango slices.

needed to achieve the end point criteria in this freezing condition were somewhat lower than those obtained for the other two freezing rates.

The temperature history of the freezing data of the assays can be used to determine the initial freezing temperature of MS, recording the rise in each sample temperature after its initial supercooling point. From this information, the average initial freezing temperature of MS was ca. -1.9 ± 0.1°C. The MS were frozen by contact with the refrigerated steel plate of the lyophilizer. Except for the assays with $T = 0$°C, when the sample reached *T*, the lower surface of MS was at least partially frozen when the VISF treatments were applied. The surface freezing is caused by the thermal demand of the sudden superficial water crystallization, which in turn is owed to the pressure differential between chamber pressure and supercooled water and/or surface ice. The effect of VISF in water solutions is the local and well-arranged surface freezing which leads to the formation of an ordered structure that allows faster sublimation during freeze-drying. Despite the presence of a solid phase (MS are a solid material, and the VISF application was done when part of its water was frozen), the use of VISF in solid samples like MS also ordered the surface structure and allowed to obtain a more dried product. This driven force is weakened as sample temperature is lower and chamber pressure is higher. That could explain the higher values of DMS final moisture content predicted by the model for $P = 900$ mtorr (Fig. 4).

Rehydration capacity

In lyophilized products, the elevated rehydration capacity values are attributed to the high porosity, which contribute to preserve the structural and cellular integrity of the fruit.[27]

In one study with acerola, the high porosity allows to consider dehydration by freeze-drying as a reversible process, resulting product with large rehydration capacity and excellent color and flavor.[28] This property is important especially in food products like cereals accompanied with dehydrated fruit and also for ready-to-eat products.[29]

Table 2 gives the results for the RC of DMS when immersed in distilled water at 25°C for 15 min. The average fresh fruit and DMS moisture content were 83.75 ± 1.93 and 4.5 ± 1.5% (wet basis), respectively. So, from water mass balance, the maximum possible value of RC for DMS was then 4.9 ± 0.1%. In general, the average measured values of RC were lower than this number and ranged between 3.3 and 3.8%. This result was similar to the findings in a study of lyophilized mango slices in which the maximum observed RC value was 3.89 after 20 min.[30]

The most significant terms in the model for the rehydration response were T ($p < 0.05$), F ($p < 0.001$) and the interaction P–F ($p < 0.01$) (Table 3). The model equation for RC predicted its highest values (4.0 ± 0.2) when $T = -4$°C, F was 0.4°C/min and P was 900 mTorr (Fig. 5).

Total color difference ΔE_{ab}

Total color difference ΔE_{ab} is a quantitative parameter used to characterize the variation of color in food processing. Depending on the value of ΔE_{ab}, differences in perceivable color between different citrus juice samples could be estimated such as not noticeable (0–0.5), slightly noticeable (0.5–1.5), noticeable (1.5–3.0), well visible (3.0–6.0), and great (6.0–12.0).[31] When it comes to fruit drying, ΔE_{ab} between the fresh and dried sample is generally greater than 12.

Freeze-drying induced color changes in the surface of fresh and dried MS. However, the fluctuations in Δa^* (redness/greenness), although being noticeable, seem to have only a minor effect on ΔE_{ab}, which seem to be more dependent on changes in ΔL^* and Δb^* (yellowness/blueness), when ΔE_{ab} was estimated from Eq. (4). All of the dried samples, excepting three, showed negative ΔL^*, indicating that DMS became darker than fresh mango. Three of four of the slices subjected to 900 mTorr of ultimate chamber pressure in VISF exhibited high degree of darkness while the same proportion of MS exposed to 500 mTorr showed negligible or positive ΔL^* changes (Table 2). This suggests that the lower the final chamber pressure during VISF treatments, the lower the change in lightness of the dehydrated mango.

In this work, the ΔEab between fresh and lyophilized fruit samples ranged from 4.39 to 22.59. A similar range for ΔE_{ab} (5–30) was found for fresh and dehydrated fruit samples that were processed by different drying

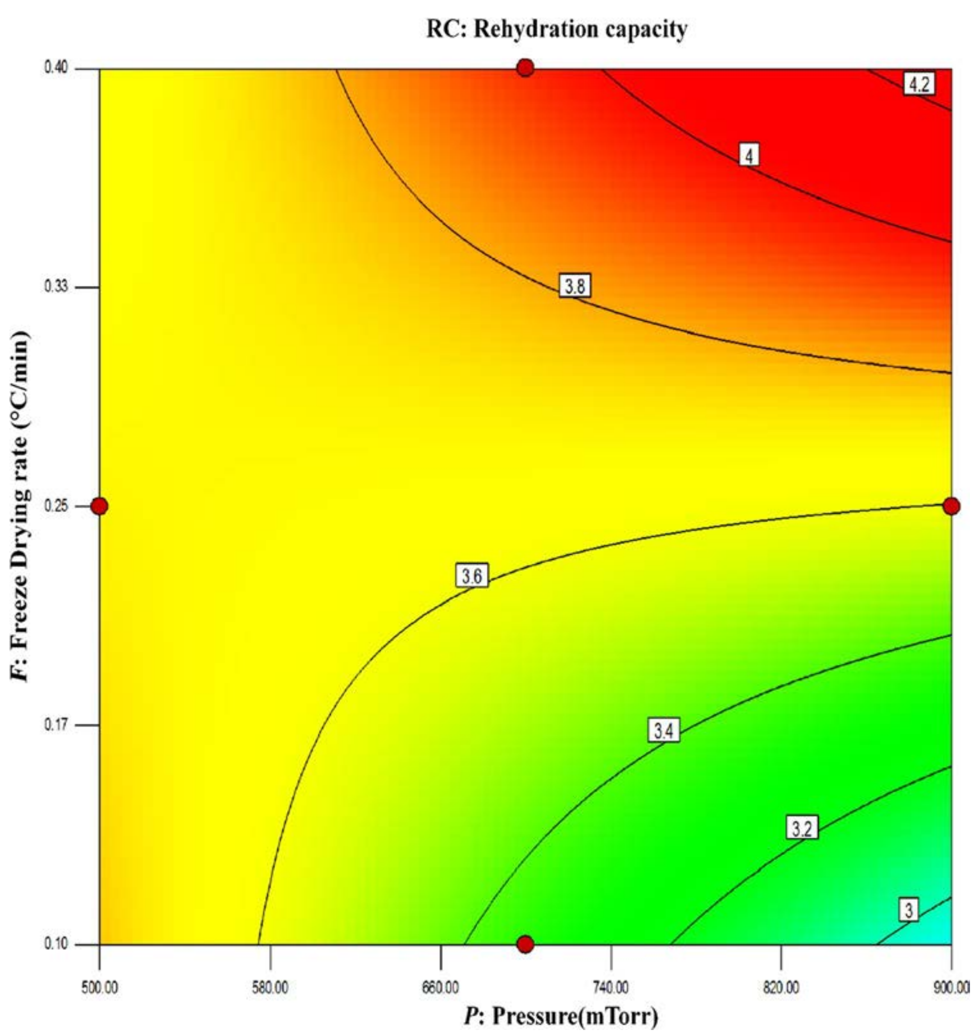

Figure 5. Contour plot showing the effects of F and P on rehydration capacity at $T = -4$°C.

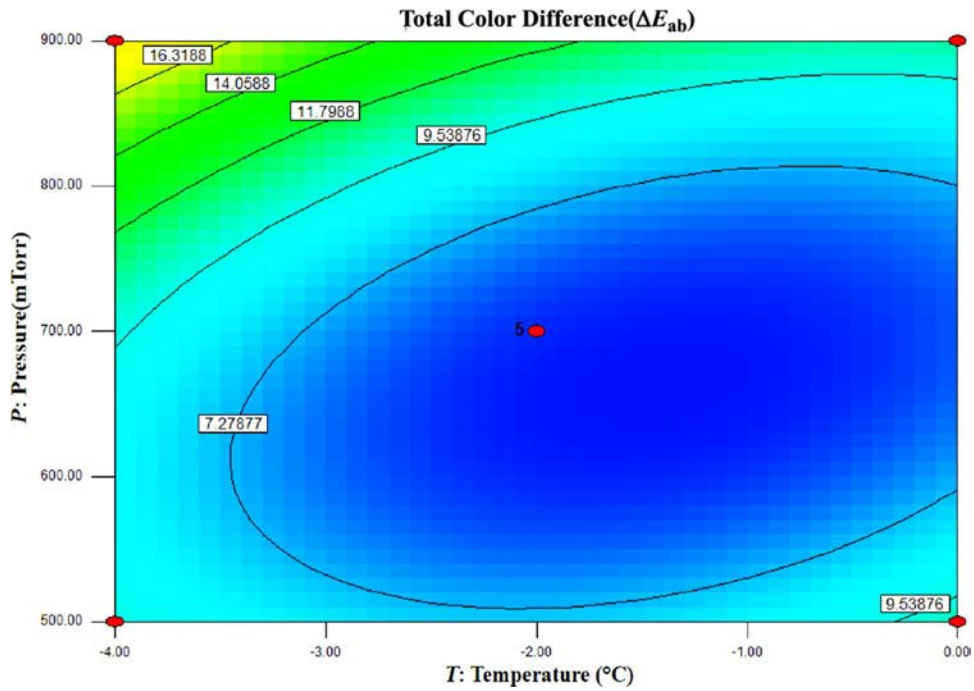

Figure 6. Contour plot showing the effects of P and T on total color difference at $F = 0.25$°C/min.

methods in works conducted by Chong et al.[32] for mangoes (ΔE_{ab} from 5 to 30) and by Rahman and Saidur[33] for strawberries (ΔE_{ab} from 3.93 to 12.75). Although there have been no studies under similar conditions of this work, one research where carrot slices were dried by combining freeze-drying with a short microwave treatment and air or vacuum drying reported that the final drying in vacuum oven had some beneficial effect on color.[34]

Analysis of variance for polynomial models for ΔL^* and ΔE_{ab} color responses showed that only the latter was suitable for the prediction of color change of MS in the applied experimental arrangement. In the modeled equation for ΔE_{ab} (Table 3), the more significant input variables were F ($p < 0.01$) and P ($p < 0.05$). For $F = 0.25$°C/min, this function produced a contour plot with more than half of all the area between contours filled with deep blue solid color, corresponding to local minimum ΔE_{ab} (Fig. 6). The $F = 0.1$°C/min plot was similar, but with a higher area for the minimum (blue filled) contour plot. Hence, the application of VISF treatment for these two F conditions gave rise to low color change of DMS, being the smallest experimental and modeled ΔE_{ab} values found at $F < 0.4$°C/min and $P < 800$ mTorr. Interestingly, the P–T area (near $P = 900$ mm and $T = -4$°C) that presented upper ΔE_{ab} is the same in which high residual moisture was detected for DMS. As mentioned earlier, when that combination of VISF conditions was applied, the MS samples had partially frozen over, and apparently, the surface structural change promoted for this treatment was partially hindered.

As smaller changes in color after the drying operation make dried products more attractive allowing keep characteristics very close to those of fresh fruit, VISF had a beneficial effect on the reduction of color changes in DMS in practically all the studied conditions. Application of VISF seems to give a relevant contribution to keep the DMS color closely to the fresh mango, which could be considered as a positive result to the potential commercialization of the dried products. The photographs in Fig. 7 clearly illustrate this.

Total polyphenol content

Polyphenols in mango have been widely studied due to their health-promoting properties through their antioxidant activity. The TPC for fresh mango was 443.29 mg GAE/g dry fruit. Results of TPCs are shown in Table 2.

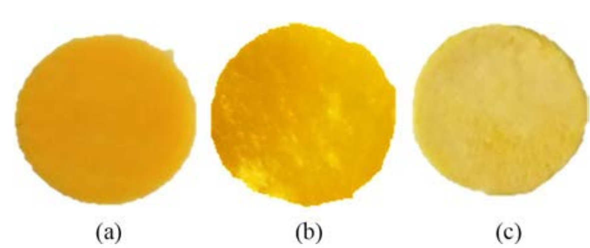

Figure 7. Qualitative color changes in MS. (a) Fresh, (b) freeze-dried with VISF and (c) freeze-dried without VISF. *Note*: VISF, vacuum-induced surface freezing.

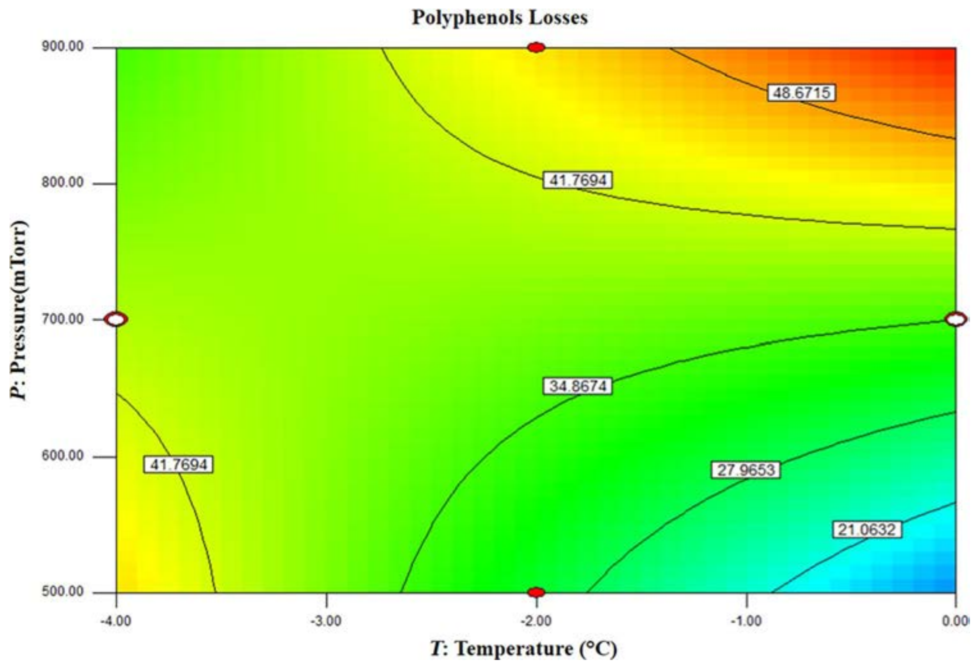

Figure 8. Contour plot showing the effects of *P* and *T* on polyphenols losses at $F = 0.25$°C/min.

However, statistical analysis was done taking into account the polyphenol losses with respect to the fresh mango values, and Table 3 shows the corresponding ANOVA results. From the results, it can be concluded that the main process variables that influenced changes in TPC were P ($p < 0.01$), F ($p < 0.05$), and $T*P$ ($p < 0.001$).

In general, drying methods affect the TPC (Fig. 8). However, Sogi et al.[35] observed the lowest TPC losses when mango samples were dried by freeze-drying. In the present work, the TPC losses were ranged between 6 and 57% (comparing with fresh mango result). To compare, a study conducted by Shofian et al.[36] reported TPC losses of 23% when mango was freeze-dried. As the highest changes in TPCs were more representative at low F (0.1°C/min), it could be attributed to enzyme activity causing degradation of some phenolic compounds.[36]

The processing temperature affects the stability of food bioactive compounds (ascorbic acid, polyphenols, and carotenoids). Polyphenols are enzymatically degraded in the presence of polyphenol oxidase (PPO) and peroxidase (POD).[37] Korbel et al.[38] studied the activity of PPO and POD in mango. They found that these enzymes are still active at lower temperature and partially active at the end of the drying process. This fact could explain the reduction in TPC of the DMS.

Energy cost estimation

According to the actual power readings, the greatest power consumption of the equipment was observed during the condenser temperature stabilization, at the beginning of freezing stage, and while the VISF treatment was performed. After the condenser temperature was achieved, the electricity consumption stabilized. Important power surges were recorded during VISF and at the start of the lyophilization stage. After the process was stabilized, the readings were approximately the same until the end of the drying.

According to TPT results, F was the variable that exhibited the highest impact in energy cost.

Table 4 shows the minimum TPT for each freezing rate and the corresponding electricity costs, calculated from Eq. (5) with a current average energy cost of US $0.12/kWh. The energy savings (%) per run with respect to the 0.1°C/min freezing rate were 26 and 33% for the 0.25 and 0.4°C/min freezing rate tests, respectively.

In general, researches about food dehydration by freeze-drying are focused on quality parameter evaluation. However, in this work, process times and energy costs are also provided, which can be useful in food industries.

Optimization

Using the response models from Table 3, a graphical optimization was performed using the Design-Expert

Table 4. Comparison of electricity costs per run at the minimum TPT for each freezing rate.

Freezing rate (°C/min)	Total process time (min)	Energy costs US$/run
0.1	1500	6.09
0.25	1145	4.52
0.4	1065	4.07

TPT, total process time.

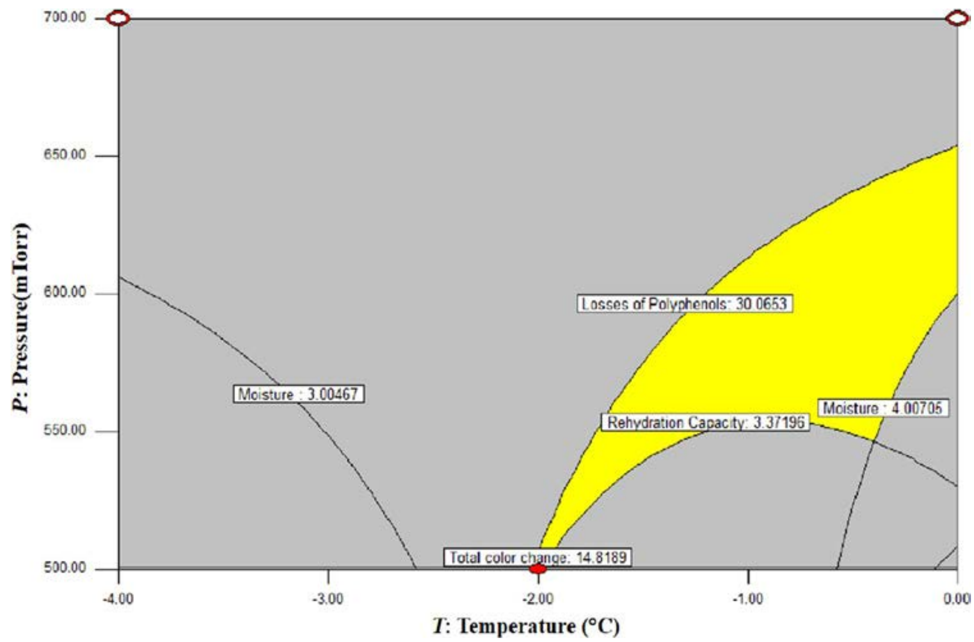

Figure 9. Overlay plot of freeze-drying optimization conditions at $F = 0.4$°C/min.

Table 5. Results obtained in the assays for validation of the conditions optimized for freeze-dried mango slices with the application of VISF.

	Process variables optimum point values[a]			Responses[b]				
Experimental assay	T	P	F	TPT	Moisture	Color	Rehydration capacity	PL
1	570	−1	0.4	1131	4.11 ± 0.23	13.68 ± 2.96	3.50 ± 0.75	33.45 ± 3.76
2	570	−1	0.4	1133	3.80 ± 0.96	11.36 ± 3.30	3.75 ± 0.25	28.69 ± 1.40
3	570	−1	0.4	1116	3.48 ± 0.67	11.51 ± 4.94	3.60 ± 0.33	30.02 ± 2.28
Average				1126.67	3.80	12.18	3.62	30.19
Criteria				<1150	3 > MC < 4	$8 > \Delta E_{ab} < 15$	3 > RC < 4	13 > TPC < 30
Results predicted by statistical analysis				1110	3.74	14.67	3.41	28.78

VISF, vacuum-induced surface freezing.
[a]P: vacuum-induced surface freezing pressure (mTorr); T: temperature at which the vacuum-induced pressure was applied (°C); F: freezing rate (°C/min).
[b]TPT: total process time (min); PL: polyphenol losses.

program. By this method, the optimal conditions are achieved by varying the sets of input parameters and visualized by overlaying the contour plots of all of the models. An appropriate final overlay plot shows a colored area where the requirements are fulfilled.

The optimization targets for DMS were (1) TPT < 1150 min; (2) moisture content between 3 and 4% (w.b.); (3) rehydration capacity of 3 to 4; (4) total color difference ΔE_{ab} between 8 and 15; and (5) total polyphenol losses between 13 and 30%. Targets 2 and 3 were chosen based on the empirically tested characteristics of commercial freeze-dried mango snacks purchased in local supermarkets. The other three objectives were derived from the experimental data in the present work.

The optimal operating conditions were determined by superimposing the contour plot as is shown in Fig. 9. To reach desirables and commercial conditions, the best areas of work could be low values of P (500–650 mTorr), T values between −2 and 0°C, and F values close to 0.4°C/min.

One optimal point ($T = -1$°C, $P = 560$ mTorr, and $F = 0.4$°C/min) was reproduced to validate the results, obtaining average values among the desirable criteria (Table 5), which demonstrates a good degree of prediction.

Conclusion

Freeze-drying of fruits is currently a commercial dehydration technology that offers delicious and healthful ready-to-eat products. Nevertheless, the production costs of freeze-dried fruits are exceedingly high compared to those of conventional air-dried fruit snacks, so that lyophilized fruits remain unaffordable products for a wide sector of the population. The results of the present work highlight how the selection of appropriate sets of operating conditions for freeze-drying mango slices can result in significant reductions in the TPT (30%), thereby lowering the energy cost and environmental impact of drying. This objective may be achieved while preserving or enhancing the product-quality characteristics.

One optimal point was reproduced to validate the results ($P = 570$, $T = -1$, and $F = 0.4$), obtaining average values among the desirable criteria of acceptability for fulfilling the commercial quality parameters ($TPT < 1150$, $3 > MC < 4$, $8 > \Delta E_{ab} < 15$, $3 > RC < 4$, and $13 > TPC < 30$).

Future work on microstructures could be done to evaluate changes in the structure of dried fruit according to each assay. On the other hand, additional studies are warranted to develop a practical guide for freeze-drying technology that would be capable of producing reasonably priced, high-quality freeze-dried food in a short time.

Funding

The authors wish to thank the financial support of COLCIENCIAS (Projects 647-2014 and 727-2015 “Apoyo a Doctorados Nacionales—Colombia” and Contract RC N° 0019-2014), DIMA (Dirección de Investigación de la Universidad Nacional de Colombia-sede Manizales), and FONTAGRO (Contract FTG/RF1330RG, Project FTG/RF - 13019).

Nomenclature

a^*	red-green dimension
AAD	absolute average deviation
Adj. R^2	adjusted R^2
AP	adequate precision
b^*	yellow-blue dimension
BBD	Box–Behnken design
DMS	dried mango slices
F	freezing rate (°C/min)
L^*	luminosity
LOF	lack of fit
m	weight
MC	moisture content (% w.b)
MS	mango slices
P	the minimum value of chamber pressure during vacuum-induced pressure treatment (mTorr)
PL	polyphenols losses (%)
POD	peroxidase
PPO	polyphenol oxidase
p-value	probability of error
RC	rehydration capacity
T	sample temperature at which the induced vacuum is applied (°C)
TPC	total polyphenols content
TPT	total process time (min)
W	power (W)
w.b.	wet basis
X	levels of response variables
Y	response function
2FI	two-factor interaction

Greek symbols

β	components
ε	standard random error
ΔE_{ab}	total color difference
Δt	stage time (min)

Subscripts

f	final
i	initial level of response variable
ii	quadratic
ij	interactive
j	final level of response variable
0	initial

ORCID

Carlos E. Orrego http://orcid.org/0000-0002-7636-878X

References

[1] Rocha, S.C.S.; Souza, J.S.; Alsina, O.L.S.; Medeiros, M.F.D. Drying of tropical fruit pulps: Spouted bed process optimization as a function of pulp composition. *Drying Technology* **2011**, *29*(13), 1587–1599.

[2] Krzykowski, S.; Dziki, A.; Polak, D.; Rudy, R. Influence of heating plates temperature on freeze drying energy requirements and quality of dried vegetables. *TEKA Commission of Motorization and Energetics in Agriculture* **2012**, *12*(2), 129–132.

[3] Devahastin, S.; Mujumdar, A.S. Indirect Dryers. In *Handbook of Industrial Drying*; Mujumdar, A.S., Ed.; CRC Press: Boca Raton, FL, 2014; 128–129.

[4] Food and Agriculture Organization of the United Nations. (2015). FAOSTAT Database. Rome, Italy: FAO. Retrieved January 30, 2016 from http://www.fao.org/faostat/en#data/QC

[5] Alvarado, J.R. Las tareas del acuerdo de la competitividad de la cadena productiva del mango. *Revista Frutas y Hortalizas* **2012**, *25*, 16–19.

[6] Ochoa-Martínez, C.I.; Quintero, P.T.; Ayala, A.A.; Ortiz, M.J. Drying characteristics of mango slices using the Refractance Window™ technique. *Journal of Food Engineering* **2012**, *109*(1), 69–75.

[7] Caparino, O.A.; Nindo, C.I.; Tang, J.; Sablani, S.S.; Chew, B.P.; Mathison, B.D.; Fellman, J.K.; Powers, J.R. Physical and chemical stability of Refractance Window®–dried mango (*Philippine “Carabao” var.*) powder during storage. *Drying Technology* **2017**, *35*(1), 25–37.

[8] Chaux-Gutiérrez, A.M.; Santos, A.B.; Granda-Restrepo, D.M.; Mauro, M.A. Foam mat drying of mango: Effect of processing parameters on the drying kinetic and product quality. *Drying Technology* **2017**, *35*(5), 631–641.

[9] Ceballos, A.M.; Giraldo, G.I.; Orrego, C.E. Effect of freezing rate on quality parameters of freeze dried soursop fruit pulp. *Journal of Food Engineering* **2012**, *111*(2), 360–365.

[10] Geidobler, R.; Winter, G. Controlled ice nucleation in the field of freeze-drying: Fundamentals and technology review. *European Journal of Pharmaceutics and Biopharmaceutics* **2013**, *85*(2), 214–222.
[11] Orrego Alzate, C.E. In *Congelación y liofilización de alimentos*; Universidad Nacional de Colombia Sede Manizales: Manizales, Caldas, Colombia, 2008; 172 p. Available at www.bdigital.unal.edu.co/7837/1/9789584444363.pdf
[12] Grajales Agudelo, L.M.; Cardona Perdomo, W.A.; Orrego Alzate, C.E. Liofilización de carambola (*Averrhoa carambola* L.) osmodeshidratada. *Ingeniería y Competitividad* **2005**, *7*(2), 19–26.
[13] Franceschinis, L.; Sette, P.; Schebor, C.; Salvatori, D. Color and bioactive compounds characteristics on dehydrated sweet cherry products. *Food and Bioprocess Technology* **2015**, *8*(8), 1716–1729.
[14] Kramer, M.; Sennhenn, B.; Lee, G. Freeze-drying using vacuum-induced surface freezing. *Journal of Pharmaceutical Sciences* **2002**, *91*(2), 433–443.
[15] Oddone, I.; Pisano, R.; Bullich, R.; Stewart, P. Vacuum-induced nucleation as a method for freeze-drying cycle optimization. *Industrial and Engineering Chemistry Research* **2014**, *53*(47), 18236–18244.
[16] Oddone, I.; Van Bockstal, P.-J.; De Beer, T.; Pisano, R. Impact of vacuum-induced surface freezing on inter- and intra-vial heterogeneity. *European Journal of Pharmaceutics and Biopharmaceutics* **2016**, *103*, 167–178.
[17] Liu, J.; Viverette, T.; Virgin, M.; Anderson, M.; Paresh, D. A study of the impact of freezing on the lyophilization of a concentrated formulation with a high fill depth. *Pharmaceutical Development and Technology* **2005**, *10*(2), 261–272.
[18] Villalpando-Guzmán, J.; Herrera-López, E.J.; Amaya-Delgado, L.; Godoy-Zaragoza, M.A.; Mateos-Díaz, J.C.; Rodríguez-González, J.; Jaubert-Garibay, S. Effect of complementary microwave drying on three shapes of mango slices. *Revista Mexicana de Ingeniera Quimica* **2011**, *10*(2), 281–290. Retrieved July 12 2017, from http://www.scielo.org.mx/pdf/rmiq/v10n2/v10n2a12.pdf
[19] Salazar, N.A.; Méndez, E.K.; Álvarez, C.; Orrego, C.E. Mango (*Mangifera indica* L.) lyophilization using vaccum-induced freezing. *World Academy of Sience, Engineering and Technology* **2015**, *9*(10), 566–570.
[20] Mothibe, K.J.; Wang, C.-Y.; Mujumdar, A.S.; Zhang, M. Microwave-assisted pulse-spouted vacuum drying of apple cubes. *Drying Technology* **2014**, *32*(15), 1762–1768.
[21] Taylor, C.L. Purple pepper plants, an anthocyanin powerhouse: Extraction, separation and characterization. Ph.D. Thesis, University of Maryland, College Park, 2014. Retrieved from http://drum.lib.umd.edu/handle/1903/15731, Available at: http://drum.lib.umd.edu/handle/1903/15731
[22] Gîtin, L.; Dinică, R.; Parnavel, R. The influence of extraction method on the apparent content of bioactive compounds in Romanian *Allium* spp. leaves. *Notulae Botanicae Horti Agrobotanici Cluj-Napoca* **2012**, *40*(1), 93–97.
[23] Quiroz-Reyes, C.N.; Aguilar-Méndez, M.A.; Ramírez-Ortíz, M.E.;Ronquillo-de-Jesus, E. Comparative study of ultrasound and maceration techniques for the extraction of polyphenols from cocoa beans (*Theobroma cacao* L.). *Revista Mexicana de Ingeniería Química* **2012**, *12*(1), 11–18.
[24] Singleton, V.L.; Orthofer, R.; Lamuela-Raventos, R.M. Analysis of total phenols and other oxidation substrates and antioxidants by means of Folin–Ciocalteu reagent. *Methods in Enzymology* **1999**, *299*, 152–178.
[25] Oddone, I.; Fulginiti, D.; Barresi, A.A.; Grassini, S.; Pisano, R. Non-invasive temperature monitoring in freeze drying: Control of freezing as a case study. *Drying Technology* **2015**, *33*(13), 1621–1630.
[26] Genin, N.; Rene, F. Influence of freezing rate and the ripeness state of fresh courgette on the quality of freeze-dried products and freeze-drying time. *Journal of Food Engineering* **1996**, *29*(2), 201–209.
[27] Marques, L.G.; Silveira, A.M.; Freire, J.T. Freeze-drying characteristics of tropical fruits. *Drying Technology* **2006**, *24*(4), 457–463.
[28] Marques, L.G.; Ferreira, M.C.; Freire, J.T. Freeze-drying of acerola (*Malpighia glabra* L.). *Chemical Engineering and Processing: Process Intensification* **2007**, *46*(5), 451–457.
[29] Duan, X.; Yang, X.; Ren, G.; Pang, Y.; Liu, L.; Liu, Y. Technical aspects in freeze-drying of foods. *Drying Technology* **2016**, *34*(11), 1271–1285.
[30] Marques, L.G.; Prado, M.M.; Freire, J.T. Rehydration characteristics of freeze-dried tropical fruits. *LWT - Food Science and Technology* **2009**, *42*(7), 1232–1237.
[31] Cserhalmi, Z.; Sass-Kiss, Á.; Tóth-Markus, M.; Lechner, N. Study of pulsed electric field treated citrus juices. *Innovative Food Science and Emerging Technologies* **2006**, *7*(1–2), 49–54.
[32] Chong, C.H.; Law, C.L.; Figiel, A.; Wojdylo, A.; Oziemblowski, M. Colour, phenolic content and antioxidant capacity of some fruits dehydrated by a combination of different methods. *Food Chemistry* **2013**, *141*(4), 3889–3896.
[33] Rahman, S.M.A.; Saidur, R. A novel atmospheric freeze dryer using simultaneous application of subzero and hot air streams using a vortex chiller. *Drying Technology* **2016**, *34*(12), 1406–1413.
[34] Litvin, S.; Mannheim, C.H.; Miltz, J. Dehydration of carrots by a combination of freeze drying, microwave heating and air or vacuum drying. *Journal of Food Engineering* **1998**, *36*(1), 103–111.
[35] Sogi, D.S.; Siddiq, M.; Dolan, K.D. Total phenolics, carotenoids and antioxidant properties of Tommy Atkin mango cubes as affected by drying techniques. *LWT - Food Science and Technology* **2015**, *62*(1), 564–568.
[36] Shofian, N.M.; Hamid, A.A.; Osman, A.; Saari, N.; Anwar, F.;Pak Dek, M.S.; Hairuddin, M.R. Effect of freeze-drying on the antioxidant compounds and antioxidant activity of selected tropical fruits. *International Journal of Molecular Sciences* **2011**, *12*(7), 4678–4692.
[37] Rawson, A.; Patras, A.; Tiwari, B.K.; Noci, F.; Koutchma, T.; Brunton, N. Effect of thermal and non thermal processing technologies on the bioactive content of exotic fruits and their products: Review of recent advances. *Food Research International* **2011**, *44*(7), 1875–1887.
[38] Korbel, E.; Servent, A.; Billaud, C.; Brat, P. Heat inactivation of polyphenol oxidase and peroxidase as a function of water activity: A case study of mango drying. *Drying Technology* **2013**, *31*(13–14), 1675–1680.